Polymer 283 (2023) 126262

Contents lists available at ScienceDirect

Polymer

journal homepage: www.elsevier.com/locate/polymer

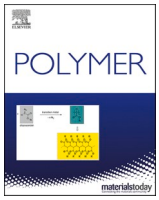

The use of lanthanide triflates in the preparation of poly(thiourethane) covalent adaptable networks

Federico Guerrero [a], Francesco Gamardella [a], Xavier Ramis [b], Silvia De la Flor [c,**], Àngels Serra [a,*]

[a] Analytical and Organic Chemistry Dept., Universitat Rovira i Virgili, C/ Marcel·lí Domingo s/n Edif, N4, 43007, Tarragona, Spain
[b] Thermodynamics Laboratory, ETSEIB Universitat Politècnica de Catalunya, Av. Diagonal, 08028, Barcelona, Spain
[c] Dept. of Mechanical Engineering, Universitat Rovira i Virgili, Av. Països Catalans, 26, 43007, Tarragona, Spain

ARTICLE INFO

Keywords:
Poly(thiourethanes)
Lanthanide triflates
Covalent adaptable networks
Recyclability
Reshapability

ABSTRACT

Covalent adaptable networks (CANs) are new polymeric materials with the mechanical properties of thermosets and the possibility of being recycled like thermoplastics. Poly(thiourethane) networks have demonstrated vitrimeric-like behavior at high temperatures due to the *trans*-thiocarbamoylation process, which Lewis acids and bases can accelerate. In this study, we report the use of lanthanide triflates (La, Sm, Dy, Er, and Yb) as Lewis acid catalysts, a greener alternative to other metallic catalysts as dibutyltin dilaurate (DBTDL) widely used in poly (urethane) and poly(thiourethane) networks. Moreover, they are not as reactive as DBTDL, and the curing mixture can be manipulated for a longer time at room temperature. As monomers, trimethylolpropane tris(3-mercapto propionate) (S3), hexamethylene diisocyanate (HDI), and isophorone diisocyanate (IPDI) have been used. We have demonstrated that the materials prepared with lanthanum triflate present the lowest relaxation times than those prepared with other lanthanide triflates or DBTDL. Calorimetry (DSC) and infrared spectroscopy (FTIR) were applied to study the curing process. The materials obtained were fully characterized by thermogravimetric analysis (TGA) and thermomechanical tests (DMA).

1. Introduction

The first report on applying lanthanide triflates as Lewis acids in organic synthesis appeared in 1987, in which triflates of different metals were tested in the reaction between amines and nitriles. [1] The main advantages of these catalysts over other Lewis acids are their commercial availability, their low toxicity, [2] their tolerance to air, moisture, and protic solvents (such as water, alcohols, and carboxylic acids), [3] and their ease of handling and recycling. Lanthanide ions have low electronegativity and strong oxophilicity, and the effect of triflate anion, with an electron-drawing capacity, increases their Lewis acidity. [4] Moreover, the Lewis acidity and the coordination ability can be modulated by changing the lanthanide metal. [5] Thus, these Lewis acids are very advantageous as they possess a higher activity and less corrosive behavior compared with Brønsted acids. [6].

It has been shown that lanthanide triflates are one of the best catalysts for ring-opening polymerization. [7–9] By this mechanism, our group reported many years ago their use in the curing of epoxy resins, [10,11] and in the copolymerization of epoxy resins with lactones. [12, 13] Other exciting applications have been their use as catalysts in C–C bond-forming reactions: aldol, Michael, allylation, Diels-Alder, Friedel–Crafts, and glycosylation. [14] Also, they can be used as precursors of chiral catalysts in asymmetric synthesis. [15] In this work, we have explored their ability to cure isocyanates with thiols and their effect on the relaxation of the poly(thiourethane) (PTUs) networks obtained to reach good recyclability.

Poly(thiourethane)s, also named poly(thiocarbamate)s, are the sulfur analogs of polyurethanes (PUs), one of the most produced polymers today (5% of the total polymer production). [16] They present some advantages in front of PUs since they are more flexible, feasible, [17,18] biocompatible, and have better optical properties with high transparency. [19] Moreover, PTUs do not present side-reactions as PU does, such as allophanate and the formation of urea groups. [20] However, PTUs are less studied than PUs, because they are formed from thiols

* Corresponding author.
** Corresponding author.
E-mail addresses: silvia.delaflor@urv.cat (S. De la Flor), angels.serra@urv.cat (À. Serra).

https://doi.org/10.1016/j.polymer.2023.126262
Received 19 April 2023; Received in revised form 5 July 2023; Accepted 8 August 2023
Available online 9 August 2023

instead of alcohols, which have a higher cost and unpleasant odor. However, after curing, the materials obtained do not have to have a bad smell. The reaction between multifunctional thiols and multifunctional isocyanate monomers to form PTU networks can be catalyzed under basic conditions (nucleophilic activation) or acidic conditions (electrophilic activation).

As basic catalysts triethylamine (TEA), 4-(N,N-dimethylamino)pyridine (DMAP), 1,4-diazabicyclo[2.2.2]octane (DABCO), [21] 1,1,3,3-tetramethyl guanidine (TMG), [22] 1,5-diazabicyclo[4.3.0]non-5-ene (DBN) and 1,8-diazabicyclo[5.4.0]undec-7-ene (DBU) [23,24] have been tested. The low pK_a of thiol groups favors their deprotonation and the nucleophilic activation with base catalyst, giving a swift attack to the isocyanate carbon. As this reaction is too fast for some technological purposes, the use of latent organic bases has been proposed, among them 1-methylimidazole (1-MI), DBU, DBN, and DMAP tetraphenylborate salts. [25].

The use of acid catalysts in PTU preparation is limited to dibutyltin dilaurate (DBTDL), although it has extended use. [19,26–28] However, there is a tendency to avoid organic tin compounds due to tin toxicity since it is a reproductive toxicant and a suspected mutagenic agent. [29] Another problem associated with DBTDL is that it starts the reaction even at room temperature, giving formulations with a short pot-life.

In a previous paper, the use of isopropyl methanesulfonate (IMS) as a source of methane sulfonic acid was studied. [30] This compound when heated at temperatures above 100 °C, releases the corresponding acid, which is the true catalyst. Thus, IMS allows easier manipulation of the prepared formulation for prolonged periods.

In the present work, we proposed the study of the catalytical activity of several lanthanide triflates (La, Sm, Dy, Er, and Yb derivatives) in the preparation of poly(thiourethane) networks compared to DBTDL. The thiol-isocyanate reaction has *click* characteristics using a basic catalyst, [25] [[,31] but in the case of an acidic catalyst, this nature is not as clear due to the possibility of side reactions. From the lanthanide triflates selected, La cation is the biggest (1.172 Å) and the less acidic (Lewis acid strength 0.343). In contrast, ytterbium is the smallest (1.008 Å) and has the highest acidity (0.416). Sm (1.098 Å, 0.380), Dy (1.052 Å, 0.396), and Er (1.033 Å, 0.392) are in between. [32].

As starting monomers, we selected trimethylolpropane tris(3-mercapto propionate) (S3), hexamethylene diisocyanate (HDI), and isophorone diisocyanate (IPDI), whose structures are depicted in Scheme 1.

The occurrence of side reactions will be explored by monitoring the curing by calorimetry (DSC) and FTIR spectroscopy, and the materials prepared will be characterized by thermal analysis.

In the last years, our group has deeply studied the vitrimeric characteristics of poly(thiourethane) networks in the presence of acid [28,30] and basic catalysts. [33] Their vitrimeric features are due to the *trans*-thiocarbamoylation process that is accelerated by these catalysts. In the present study, we have studied the effect of the lanthanide triflates on the relaxation behavior of these materials by thermomechanical tests (DMA) to look for a greener and more effective catalyst for the reshaping and recycling of these materials.

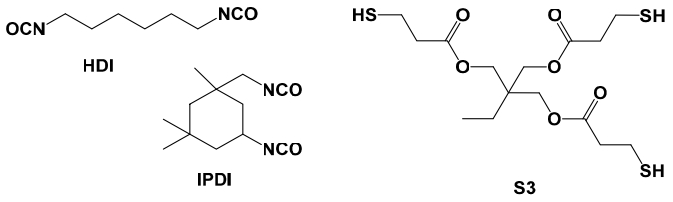

Scheme 1. Structure of the starting monomers.

2. Experimental part

2.1. Materials

Trimethylolpropane tris(3-mercapto propionate) (S3), hexamethylene diisocyanate (HDI), dibutyl tin dilaurate (DBTDL), $La(OTf)_3$, $Sm(OTf)_3$, $Dy(OTf)_3$, $Er(OTf)_3$, and $Yb(OTf)_3$ from Sigma Aldrich have been used as received. Isophorone diisocyanate (IPDI) was purchased from Acros Organics. Acetone from Scharlab was purified by distillation and dried.

2.2. Preparation of the formulations

S3 and HDI or IPDI were mixed in stoichiometric proportions: 2 mol of trithiol for 3 mol of diisocyanate. The amount of catalyst was calculated in molar percentage of the corresponding catalyst by 100 mol of thiol. First, the selected lanthanide triflate and diisocyanate were manually stirred and dissolved with the necessary amount of dry acetone. Then, the acetone was eliminated under reduced pressure at room temperature, S3 was added, and the mixture was manually stirred until complete homogenization. The formulations and materials have been named according to the following nomenclature "HDI or IPDI + lanthanide + concentration".

2.3. Preparation of the materials

The materials were prepared using a Petri dish covered with an adhesive Teflon sheet. The prepared formulation was spread on the Teflon surface and placed in an oven at 80 °C (1 day), at 120 °C and 140 °C (1 h at each temperature), and 2 h at 160 °C. After curing, samples were demolded while still hot.

2.4. Calorimetric study

A differential scanning calorimeter (DSC) Mettler DSC-3$^+$ calibrated using an indium standard (heat flow calibration) and an indium-lead-zinc standard (temperature calibration) was used to analyze the curing evolution.

Mixture quantities of approximately 5–10 mg were tested in aluminum pans with a pierced lid in an inert atmosphere (N_2) with a 50 cm^3/min gas flow. The dynamic studies were performed in a temperature range of 0–250 °C with a heating rate of 10 °C/min. The glass-transition temperatures (T_gs) of the cured materials were determined by heating a small piece of cured material between 0 and 250 °C at 20 °C/min. Enthalpies and glass transition temperatures were calculated with the help of the STARe software.

2.5. Thermal stability

The thermal stability of the cured samples was evaluated by thermogravimetric analysis (TGA) using a Mettler Toledo TGA2 thermobalance. All experiments were performed under an inert atmosphere (N_2 at a flow of 50 cm^3/min). Pieces of 10–15 mg of cured samples were degraded between 30 and 600 °C, with a heating rate of 10 °C/min.

2.6. Infrared spectra

Fourier-transform infrared (FTIR) spectra were recorded with a spectrometer Jasco FTIR 6700, in absorbance mode, with a resolution of 4 cm^{-1}, in the wavelength range from 650 to 4000 cm^{-1}, and with 32 scans of each spectrum. The instrument is equipped with an attenuated total reflection accessory (ATR) Specac Golden Gate with controlled temperature. This equipment has also been used in a kinetic mode, registering spectra every 30 s at a fixed temperature (80 and 140 °C) to get conversion-time graphs.

2.7. Viscoelastic and thermo-mechanical properties

The viscoelastic and thermomechanical properties were evaluated using a DMA Q800 analyzed from TA Instruments using a film tension clamp. Cured samples were die-cut in about 20 mm × 5 mm rectangular areas.

The evolution of tan δ and storage modulus with the temperature was investigated at a heating rate of 2 °C/min from −25 to 175 °C, at 1 Hz and 0.1% strain.

Tensile stress relaxation tests were conducted using samples with the dimensions previously defined. The samples were equilibrated at 165 °C and left at this temperature for 5 min. Then, a constant strain of 1.5% was applied (to ensure the materials were within the linear range), and the consequent stress level was measured as a function of time for 90 min. Then, the temperature was increased 5 °C, and the process was repeated until we reached the final temperature of 185 °C. Relaxation stress $\sigma(t)$ was normalized to the initial stress (σ_o), and the characteristic relaxation time (τ^*) was determined as the time necessary to relax $0.37\sigma_o$. The Maxwell equation correlates the viscosity and the relaxation time at this relation ($0.37\sigma_o$), as given in the next equation:

$$\eta = E'\cdot\tau^* \tag{1}$$

where η is the viscosity, E' is the storage modulus in the rubbery state (assuming E′ being relatively invariant in this state), and τ^* is the characteristic relaxation time. The relaxation times, τ^* obtained at each temperature are then plotted to verify that τ^* (and consequentially $\boldsymbol{\eta}$) follow an Arrhenius relationship.

$$\tau^* = \tau_0 \cdot e^{\left(\frac{E_a}{RT}\right)} \tag{2}$$

where τ_0 is the characteristic relaxation time at infinite T, E_a is the activation energy of the bond exchange reaction, R is the universal gas constant, and T is the temperature. Rewriting Eq. (2) as follows:

$$\ln \tau^* = \ln \tau_0 + \frac{E_a}{RT} \tag{3}$$

The activation energy (E_a) can be calculated directly from the slope of the representation of ln (τ*) in front of $1/T$. The topology freezing transition temperature (T_v), which describes the characteristic transition from a viscoelastic solid to a viscoelastic liquid, is calculated by substituting the value of viscosity of 10^{12} Pa s (liquid to solid transition) and E' in the Maxwell equation, thus obtaining the relaxation time (τ^*) needed to reach this viscosity. Then the extrapolated value of τ^* is substituted in the Arrhenius relationship to calculate the hypothetical T_v.

2.8. Tensile tests

Tensile strength tests were performed in dog-bone Type V samples at room temperature, using an electromechanical universal testing machine UTS Shimadzu AGS-X (Shimadzu Co., Kyoto, Japan) with a 1000 N load cell at 5 mm/min according to ASTM D638-14 standard. Three samples of each material were tested, and the average results are presented.

2.9. Recycling

The recycled samples were obtained by cutting the crosslinked polymer into small pieces and hot-pressing at 15 MPa into an aluminum mold at 190 °C for 3 h. Recycled samples were die-cut in dog-bone shapes from the new film obtained and were tested by DMA (to obtain the thermomechanical properties) and Universal Test Machine (to obtain the tensile strength). By FTIR, the permanence of the chemical structure was confirmed.

3. Results and discussion

3.1. Calorimetric study of the curing

The catalytical activity of lanthanide triflates in the reaction between S3 and the different diisocyanates (HDI and IPDI) was investigated by DSC, and the obtained curves for HDI formulations are shown in Fig. 1. The most significant data extracted from DSC tests are collected in Table 1. Stoichiometric formulations of comonomers were used to reach the highest crosslinking density. The different catalysts were added in the percentage of mol of the catalyst to mol of thiol to compare their catalytical activities without the effect of their different molecular weights.

In Fig. 1, we can observe different shapes of the DSC curves of the curing process of HDI samples, depending on the catalyst. The curves present two more or less defined peaks in formulations with lanthanide triflates. The first is at about 80 °C, and the second is at a much higher temperature depending on the lanthanide selected. The presence of these two peaks indicates that two different chemical processes occur. In contrast, the formulation containing DBTDL as the catalyst shows only one peak, indicating a more straightforward curing process.

As we can see, the enthalpy released in the first peak increases as the lanthanide triflate goes from Yb to La, following the left direction in the periodic table. Thus, the reactive process associated with this peak occurs predominantly in the lanthanum salt and less in the case of ytterbium.

Whereas the temperature of the first peak practically does not change with the catalyst, the maximum temperature of the second peak depends on the lanthanide triflate employed, as seen in Table 1. Thus, this process occurs at a higher temperature as the lanthanide used goes to the right in the lanthanide series. However, little influence is observed on the enthalpy released in the second peak by varying the lanthanide salt. It is well known that Yb is the cation with a higher Lewis acidity due to its small ionic radium. [4,34] From this point of view, the curing process would be expected to occur at lower temperatures when the ytterbium catalyst was used, which was not observed. The contrary behavior could be related to the coordination ability, which decreases going from La to Yb salts. [35] However, the coordination ability is somewhat complex and depends on the ligand. Therefore, it is not easy to predict. If the coordination ability plays an important role, this could also be related to the appearance of the exotherm at about 80 °C, more significant for

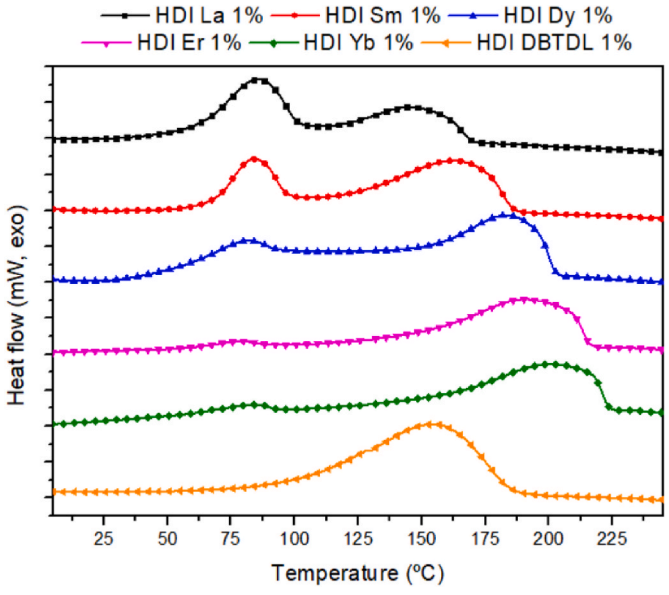

Fig. 1. DSC curves for the curing of S3-HDI formulations catalyzed by the different lanthanide triflates tested and DBTDL.

Table 1
Temperature of the maximum of the 2nd exotherm and glass transition temperature for all the formulations studied containing 1% molar of catalyst.

Catalyst	HDI		IPDI	
	T_{max} (°C)	T_g (°C)	T_{max} (°C)	T_g (°C)
$La(OTf)_3$	146	32	192	100
$Sm(OTf)_3$	162	29	194	96
$Dy(OTf)_3$	183	27	199	94
$Er(OTf)_3$	191	25	200	91
$Yb(OTf)_3$	201	25	210	90
DBTDL	155	36	185	109

lanthanum-catalyzed formulations.

When HDI was replaced by IPDI (Fig. 2), the peaks came out wider due to the different reactivity of the two isocyanate groups, which did not happen with the HDI, and the two peaks did not come out well-defined. In these formulations, the peak at a lower temperature can be observed only in samples with La and Sm triflates. The main exotherm appears at a higher temperature than in HDI formulations, which can be explained by the minor reactivity of IPDI, which is more rigid than HDI. The differences observed in the calorimetric curves of the curing process with both isocyanates could be related to differences in the coordination ability of the lanthanide to the isocyanate group. The higher steric hindrance of the isocyanates in the IPDI could difficult this coordination.

We determined the glass transition temperatures of all the materials prepared by DSC. As shown in Table 1, the highest T_g was obtained when using DBTDL as the catalyst. From the lanthanide triflates tested, the T_gs decreased from La to Yb for both diisocyanates. The higher rigidity of the IPDI monomer leads to higher T_g values for these materials, as expected. All these observations could indicate that lanthanum cation, with a bigger size, coordinates much better than ytterbium, increasing both T_gs and reactivity. Moreover, the formation of isocyanurate rings, which are rigid crosslinking points, and are formed to a different extent in the lanthanide salts tested, can also affect this characteristic temperature.

3.2. Study of the chemical reactions involved in the curing process

We monitored the curing process of the different formulations prepared by Fourier-transform infrared spectroscopy (FTIR-ATR) to determine the reactions during curing. Firstly, we compared the FTIR spectra of the HDI initial formulation catalyzed by $La(OTf)_3$ and the cured material. As shown in Fig. 3, the new peaks confirmed the only appearance of the thiourethane groups expected (bands at 3400 and 1650 cm^{-1}) and the disappearance of the isocyanate band at 2250 cm^{-1}. Thiol absorption is very weak, but it can only be perceived at 2570 cm^{-1} in the spectrum of the initial formulation. The spectrum of the cured sample does not differ from the one obtained when DBTDL was used as the catalyst.

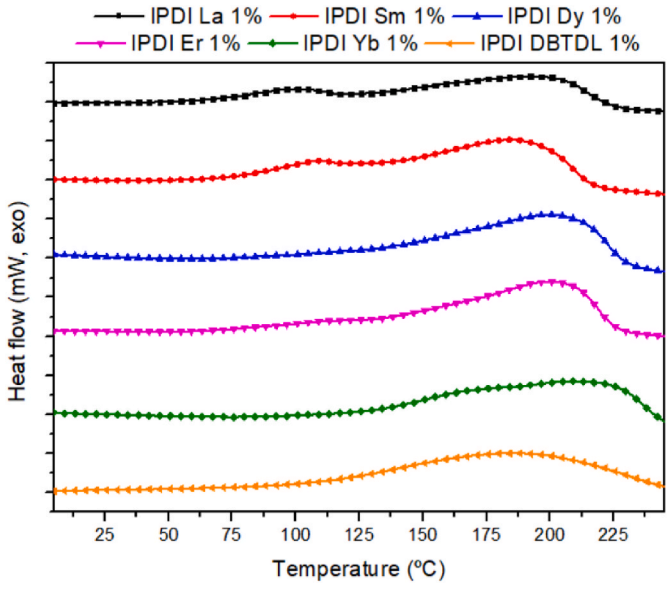

Fig. 2. DSC curves for the curing of S3-IPDI formulations catalyzed by the different 1% molar of lanthanide triflates and DBTDL.

The kinetic study of the curing process using lanthanum and ytterbium triflates was performed by ATR-FTIR at two different temperatures, 80 and 140 °C, which are the temperatures at which both curing exotherms appear, to see the differences among both formulations. The conversion was calculated using the area of the NCO stretching peak at 2250 cm^{-1}, taking the area of the carbonyl ester band of the thiol structure as the reference by the following equation:

$$\%\ \text{CONVERSION (NCO)} = \frac{\frac{Ao\ (NCO)}{Ao\ (C{=}O)} - \frac{A\ (NCO)}{A\ (C{=}O)}}{\frac{Ao\ (NCO)}{Ao\ (C{=}O)}} 100 \quad (4)$$

where A_0 is the initial area of the corresponding peak, and A is the area at each temperature. The absorbances were normalized with that of the ester group of S3 at 1730 cm^{-1}. Fig. 4 shows the conversion evolution for HDI and IPDI formulations.

In the first part of the conversion plot, we see that the isocyanate disappearance is much faster when $La(OTf)_3$ is the catalyst, especially in HDI formulations. However, $Yb(OTf)_3$ induces a slower reaction and does not generate significant differences between HDI and IPDI formulations. Thus, the use of lanthanum leads to a notable consumption of the isocyanate groups at 80 °C, where the first exothermic peak appeared in the DSC curves. Once the temperature increases to 140 °C, the disappearance of the isocyanate occurs very fast in all formulations, indicating that the formation of thiourethane functions is complete.

Analyzing in more detail the evolution of the FTIR bands along the curing process, we could detect the formation of a band at 1680 cm^{-1} when curing at 80 °C that is being displaced to a lower wavenumber (1650 cm^{-1}) on increasing the temperature up to 140 °C, as it can be observed in Fig. 5.

The band at 1680 cm^{-1} could be assigned to the stretching of the carbonyl group of isocyanurates, formed by trimerization, as represented in Scheme 2.

In a previous work of our group, we could see that on curing epoxy isocyanate formulations with lanthanide triflates as the catalyst, isocyanurates were also formed. [36] Thus, it seems that the coordination of the lanthanum cation, the biggest one, to the isocyanate favors the trimerization that takes place at moderate temperatures of 80 °C, where

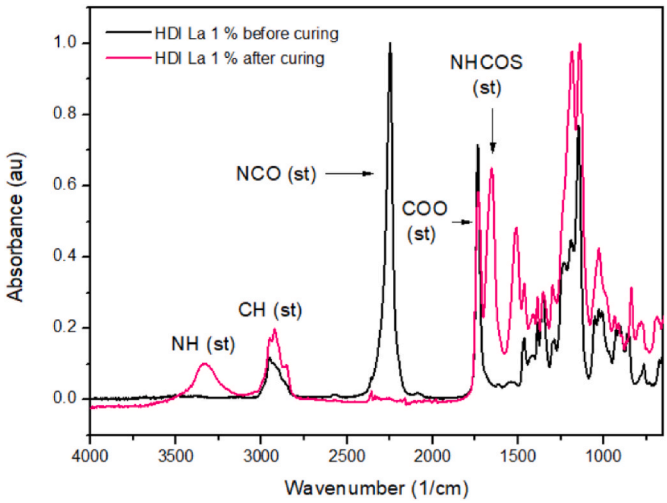

Fig. 3. FTIR spectra of the sample HDI La 1% before and after curing.

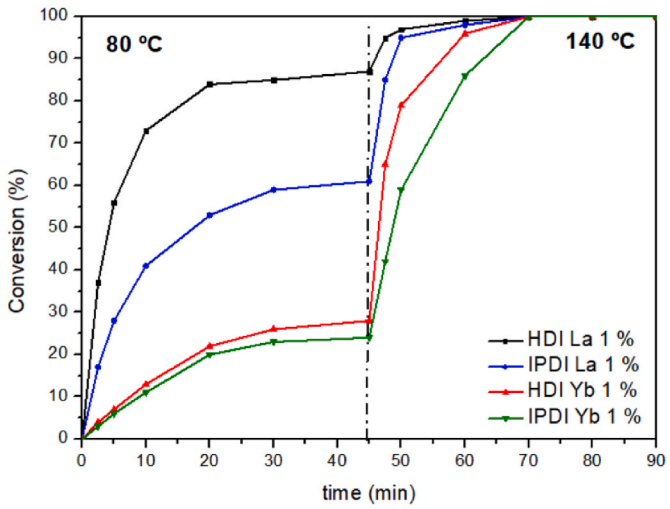

Fig. 4. Kinetic profiles of HDI and DPID formulations with 1% of lanthanum and ytterbium triflates as the catalyst at two different temperatures.

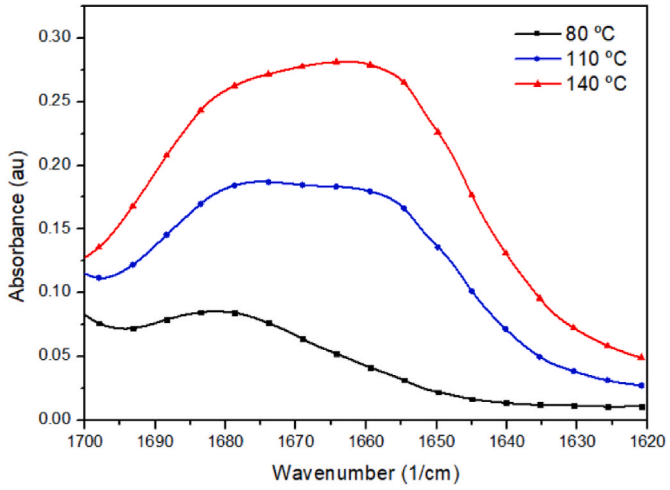

Fig. 5. FTIR-ATR curves of the curing of HDI La 1% formulation at several temperatures.

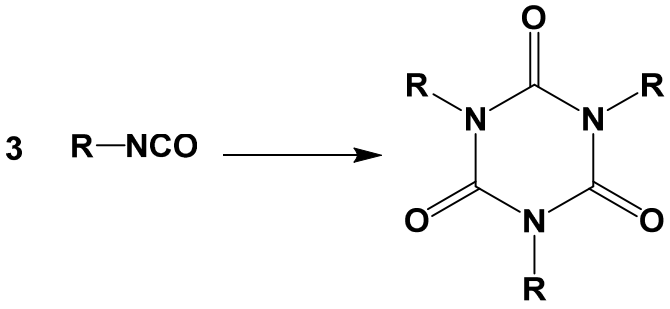

Scheme 2. Formation of isocyanurates from the isocyanate monomers.

the first exothermic peak of the DSC appears. The reversion occurs by increasing the temperature, and the isocyanate released reacts with thiols to form the corresponding thiourethane group. On reducing the size of the lanthanide cation, the coordination ability is reduced, and the formation of the isocyanurates seems less favored, as proved by FTIR and DSC studies. When DBTDL was used as a catalyst, no peak at 1680 cm^{-1} appeared, but only the expected thiourethane carbonyl st. band at 1650 cm^{-1}.

3.3. Evaluation of the thermal stability

The thermal stability of the poly(thiourethane) thermosets prepared was evaluated by thermogravimetry, and the main data extracted are collected in Table 2. Fig. 6 shows the plots of the weight loss and their derivatives of all the samples prepared with 1% of each catalyst. The evaluation of the thermal stability of the materials is of great importance to avoid the degradation of the materials in the recycling process.

From the initial degradation temperatures, we can confirm that the materials can stand the usual temperatures at which the recycling process is performed (<200 °C). No significant differences are observed among the materials prepared with lanthanide triflates, although there is a slight trend. While lanthanum salt leads to degradation at a lower temperature, when Yb triflate is used, the degradation starts at higher temperatures. The materials obtained with DBTDL begin their degradation at comparable temperatures, although slightly higher.

The DTG curves of the materials containing lanthanide triflates as the catalyst show three main degradation peaks, similar to those of the materials with DBTDL, although somewhat displaced according to the different catalyst efficiency for the degradation processes. The first step is attributed in the literature to the reversion of thiourethane to isocyanate and thiol. [37–39] The second process is associated with the β-elimination of the ester group, and the third process is due to the complete degradation of the network. Thus, there are no mechanistic differences among the materials with the lanthanide salts.

3.4. Thermomechanical characterization

The materials prepared with lanthanum and ytterbium triflates were characterized by DMA to evaluate the thermomechanical properties and to compare them to the same systems but using DBTDL as the catalyst. Fig. 7 shows the evolution of tan δ and storage moduli with temperature for HDI and IPDI materials. The main data extracted are collected in Table 3.

As shown in Fig. 7, the main difference is due to the diisocyanate structure (HDI is the more flexible, and IPDI is the one with a higher rigidity). However, the catalyst used has some influence on the thermomechanical behavior. The use of DBTDL leads to the highest tan δ temperature, and the ytterbium salt leads to the lowest. It is also worth pointing out that all the materials show unimodal curves. However, DBTDL presents the thinnest one (smaller FWMH), indicating a more

Table 2
Thermogravimetric data of all the materials prepared, and degraded in N_2 atmosphere.

Sample	$T_{5\%}$[a] (°C)	T_{max}[b] (°C)	Char Yield[c] (%)
HDI La 1%	256	281/322/400	4.0
HDI Sm 1%	260	280/321/396	4.2
HDI Dy 1%	265	279/321/392	4.4
HDI Er 1%	267	278/320/387	4.6
HDI Yb 1%	267	276/320/386	4.8
HDI DBTDL 1%	268	306/344/452	4.9
IPDI La 1%	265	285/329/393	4.5
IPDI Sm 1%	269	283/327/390	4.6
IPDI Dy 1%	271	281/327/385	4.7
IPDI Er 1%	271	277/327/378	4.9
IPDI Yb 1%	271	277/325/376	5.1
IPDI DBTDL 1%	288	288/328/420	5.2

[a] Temperatures of initial degradation (5% of weight loss).
[b] Temperatures of the maximum degradation rates of the three steps.
[c] Remaining weight percentage at 600 °C.

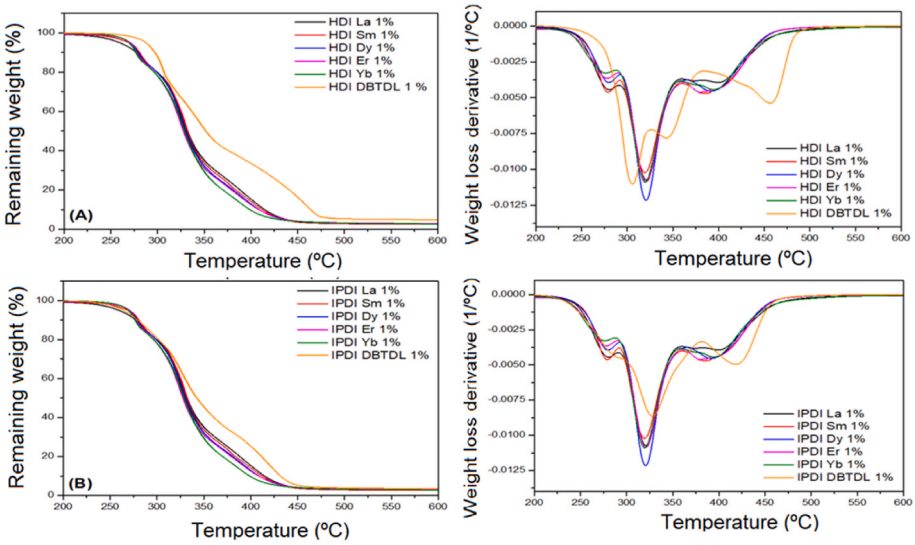

Fig. 6. TGA and DTG curves of the samples with HDI (A) and IPDI (B) with the different catalysts, recorded at 10 °C/min in the N_2 atmosphere.

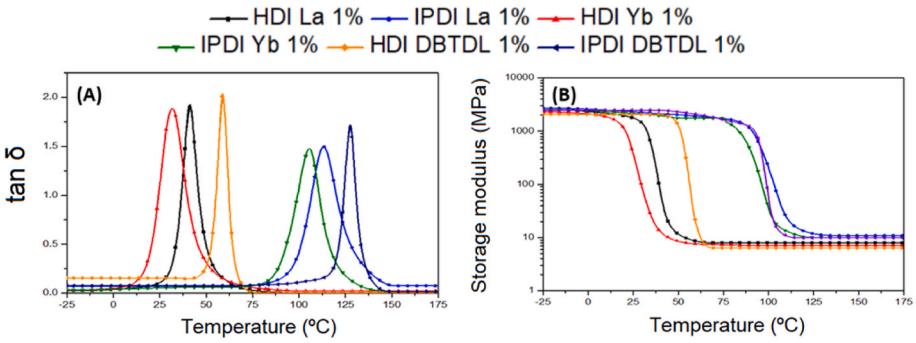

Fig. 7. Dependence of tan δ (A) and storage moduli (B) with the temperature of the different poly(thiourethane)s prepared by using 1% of different catalysts.

Table 3
Main data extracted from DMA analysis of several materials prepared.

Sample	$T_{tan\ \delta}$ [a] (°C)	FWHM[b] (°C)	E_{glassy} [c] (MPA)	$E_{rubbery}$ [d] (MPA)
HDI La 1%	42	11.5	2500	8.0
IPDI La 1%	113	13.1	2699	10.9
HDI Yb 1%	32	16.0	2283	7.1
IPDI Yb 1%	106	17.9	2540	10.1
HDI DBTDL 1%	57	10.3	2083	6.4
IPDI DBTDL 1%	132	12.5	2496	9.9
HDI La 0.5%	43	10.8	2401	7.3
HDI La 2%	41	12.4	2584	9.3

[a] Temperature of the maximum of the tan δ peak.
[b] Full width at half maximum of the tan δ peak.
[c] Storage modulus obtained at the temperature of the maximum of tan δ peak -30 °C.
[d] Storage modulus determined at the temperature of the maximum of tan δ peak +30 °C.

homogeneous structure in the materials obtained with this catalyst. This is usually related to the inexistence of side reactions, as we saw in our previous studies. [38].

Storage moduli in the rubbery and glassy states are slightly higher for IPDI-derived materials due to the higher rigidity of this structure. There are no significant differences in the rigidity of the materials when using lanthanide triflates or DBTDL as catalysts.

Since the amount of catalyst significantly affects the rate of relaxation phenomena, we studied the influence of the proportion of lanthanum triflate in the thermomechanical characteristics of these materials. As we selected 1% mol of catalyst to thiol for the study, we reduced this proportion to 0.5% and increased it to 2%. Their thermomechanical characteristics are presented in Table 3. Whereas the maximum of the tan δ is similar for all the samples, increasing the amount of catalyst slightly increases the broadness of the curves and the storage moduli in the rubbery and glassy states, being these variations not significant.

3.5. *Vitrimeric characterization*

In previous papers of our group, we reported that *trans*-thiocarbamoylation reaction could proceed at elevated temperatures in the presence of acidic and basic catalysts. The higher the proportion of catalyst, the quicker the relaxation process at the proper temperature. We demonstrated that this type of material had a vitrimeric-like behavior with the dissociation of the thiourethane group to isocyanate and thiol and a very fast reforming, as can be seen in Scheme 3, that led to a diminution of the viscosity on heating that follows an Arrhenius type evolution. [28,32,38].

To investigate the effect of the monomer structure of the different PTUs prepared and the ability of the acidic catalyst present in the material on the stress relaxation behavior, we have performed several stress relaxation experiments by DMA. We selected lanthanum and ytterbium triflates because they are the most different, and we included DBTDL as the reference in the study. The temperatures selected were well above the T_g to allow a certain movement of the network structure to perform the exchange process. Fig. 8 shows the stress relaxation curves registered at 180 °C, and the main data extracted from this study are presented in

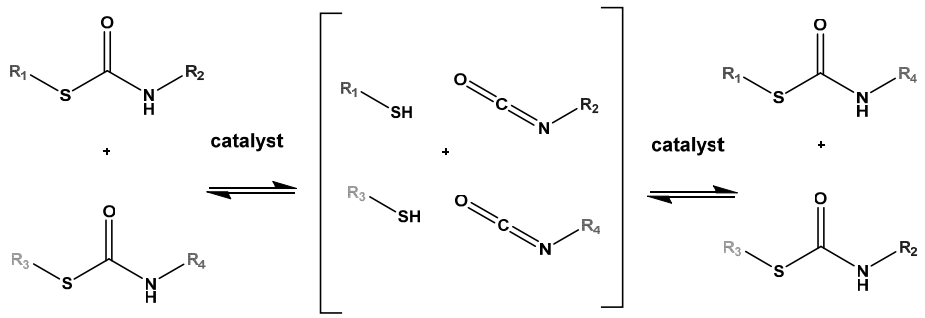

Scheme 3. Proposed mechanism of *trans*-thiocarbamoylation exchange process.

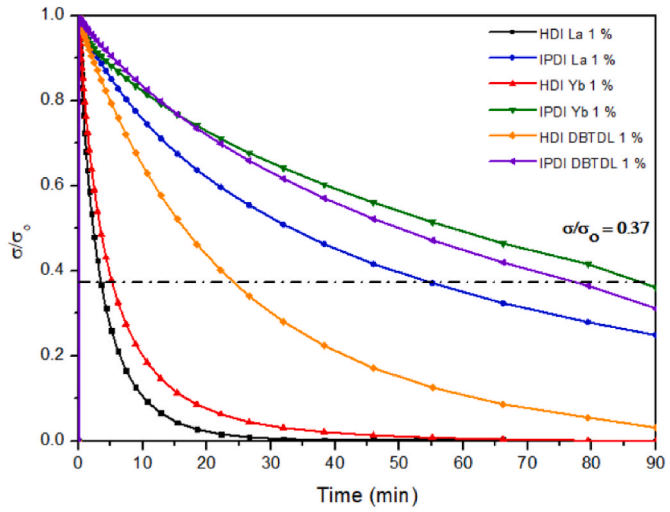

Fig. 8. Normalized stress relaxation curves at 180 °C for some PTUs prepared with 1% of catalyst.

Table 4
Main data extracted from stress relaxation experiments.

Sample	$\tau_{0.37}$[a] (min)	E_a[b] (kJ/mol)	lnA (min)	r [2]	T_v[c] (°C)
HDI La 1%	3.5	131	29.5	0.9991	115
IPDI La 1%	55.5	137	30.7	0.9990	119
HDI Yb 1%	5.5	125	24.7	0.9933	139
IPDI Yb 1%	88.5	126	25.2	0.9999	146
HDI DBTDL 1%	24	117	26.2	0.9949	135
IPDI DBTDL 1%	78	121	27.9	0.9961	139
HDI La 0.5%	10.7	155	27.0	0.9976	122
HDI La 2%	1.5	126	36.6	0.9990	113

[a] Time to reach a value of $\sigma/\sigma_o = 0.37$ at 180 °C.
[b] Activation energy of the exchange process.
[c] Topology freezing transition temperature.

Table 4.

As we can see, the materials obtained from HDI prepared with the lanthanum salt are the ones that relax faster, followed by the ytterbium triflate. The complete relaxation of HDI materials was reached in less than 40 min when using 1% of the lanthanum salt as the catalyst (70 min with ytterbium). In contrast, when using DBTDL or IPDI structure, the materials needed more than 90 min to relax the stress completely. The differences are not as noticeable when using IPDI as the monomer, but lanthanum triflate also leads to faster relaxation.

Compared to DBTDL, lanthanum salt leads to the best results in the relaxation of the stress and, as discussed before, in the kinetics of curing, presenting similar thermomechanical characteristics. This behavior can be attributed to the size of the lanthanum cation that leads to the best conjunction of Lewis acidity and coordination capacity.

We also investigated how changing the amount of lanthanum triflate affects the relaxation ability. The reduction to 0.5% increases the time to reach $\tau_{0.37}$–10.7 min, whereas on increasing the proportion up to 2%, this time was reduced to 1.5 min. 1% of $La(OTf)_3$ is less than 3 phr (parts per hundred of thiol), whereas 4 phr of DBTDL were needed in previous work to reach a $\tau_{0.37}$ of 20 min. [28] The values of $\tau_{0.37}$ are of the same magnitude as those reported using basic organocatalysts (tetraphenylborate salts of amidine compounds such as DBN, DBU, and TBD). [32] The advantage of the lanthanum salt when catalyzing the relaxation of PTUs is that it is commercially available, allows the storage and manipulation of the formulations several times (in contrast to DBTDL and other non-latent basic catalysts), and the materials obtained are more stable at higher temperatures than the ones obtained with organocatalysts, which begins to degrade at temperatures around 210 °C.

To calculate the kinetic parameters of the stress relaxation phenomena using the new catalyst, we performed stress-relaxation experiments at different temperatures for each type of material. As shown in Fig. 9, for the sample HDI with 2% of $La(OTf)_3$, the relaxation time is clearly dependent on the temperature.

From the values of $\tau_{0.37}$ at each temperature, the Arrhenius plots were constructed for all the systems studied. Fig. 10 presents the evolution of these values against the inverse of the temperature. The activation energies and the adjusting parameters are included in Table 4.

The fact that the evolution of the viscosity of the materials with lanthanide triflates with time follows an Arrhenius evolution helps us to assert that the PTUs prepared to have a vitrimer-like behavior as

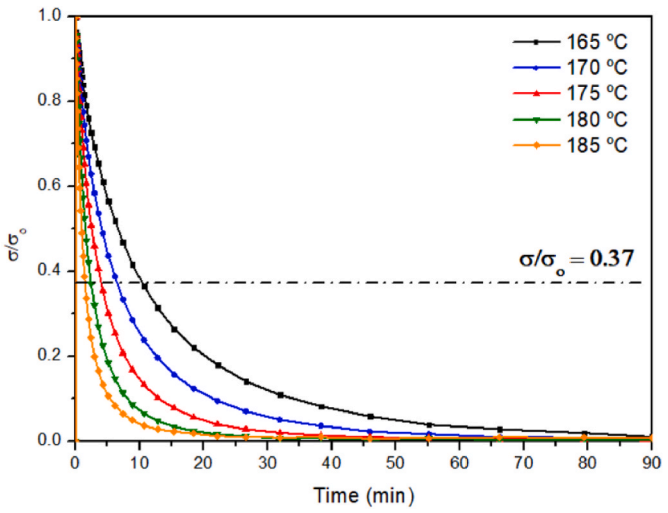

Fig. 9. Normalized stress relaxation curves as a function of time at several temperatures from 165 to 185 °C during 90 min for the sample HDI La 2%.

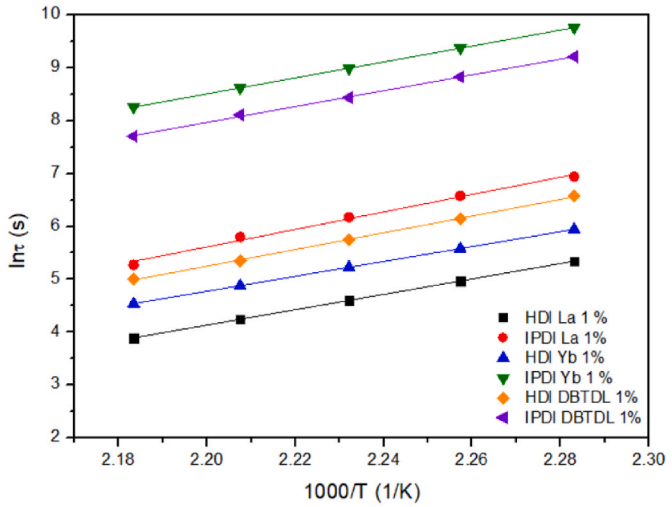

Fig. 10. Arrhenius plot of relaxation times against inverse temperature for the materials with different catalysts, obtained from relaxation experiments.

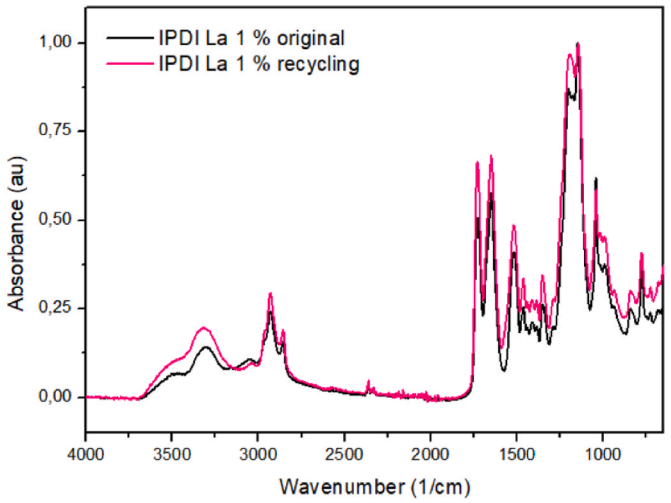

Fig. 12. FTIR spectra of the IPDI 1% La virgin material and after the recycling process.

reported previously since these catalysts are very effective in the reaction of isocyanates with thiols but also in the decomposition of thiourethanes to isocyanate and thiols. [32] Although the activation energies calculated for the lanthanum salt are higher than those for ytterbium and DBTDL, the higher values of the pre-exponential factor lead to the fastest relaxation. On increasing the proportion of the lanthanum salt in the mixture, the activation energy decreases, as observed previously for DBTDL. [28].

The different T_vs (topology freezing transition temperatures), the temperature at which the materials reach a viscosity of 10^{12} Pa s, were calculated from the Arrhenius plot, and the values were also included in Table 4. The calculated T_vs for each material are above $T_{tan\ \delta}$; therefore, the $T_{tan\delta}$ has to be overpassed to reach the reorganization of the network. It has to be commented that although the correlation in the Arrhenius plots is excellent, little errors in the activation energies produce significant deviations in the relaxation times and, consequently, in the T_v calculated. The lanthanum salt leads to the lowest T_v for materials derived from HDI and PDI, and the increase in its proportion reduces this temperature.

3.6. Recycling

To confirm the recyclability of the materials prepared, we selected the IPDI La 1%. The material was cut into small pieces and hot-pressed at 15 MPa in an aluminum mold at 190 °C for 3 h, since this temperature combines a fast relaxation process with the thermal stability tested by TGA and confirmed in isothermal conditions at this temperature. Fig. 11 shows the good appearance and transparency of the material after recycling.

The recycled material was examined by FTIR spectroscopy and compared with the virgin one. Fig. 12 shows the FTIR spectra, showing

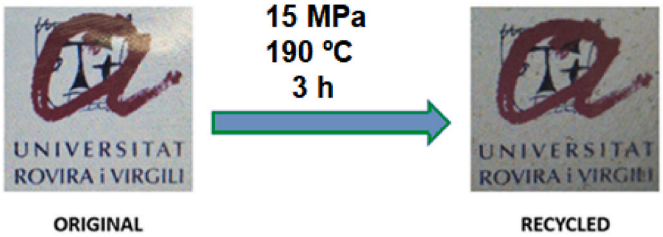

Fig. 11. Photographs of the original and recycled IPDI La 1% sample showing the high transparency of the recycled material.

that the chemical structure remains unchanged after recycling.

The recycled material was also tested by DMA to assess the thermomechanical properties of the recycled material. Fig. 13 shows the evolution of the storage moduli and tan δ with temperature, where no significant differences can be appreciated, confirming these materials' good recyclability.

We also performed tensile tests on the original and recycled sample to compare their stress-strain behavior. To do that, samples were die-cut in dog-bone shapes and tested in the UTS Shimadzu AGS-X. Three samples were tested, and the average results are presented in Table 5.

As we can see from the mechanical parameters extracted from the tensile tests, sample IPDI with 1% of $La(OTf)_3$ behaves quite similarly before and after recycling. The stiffness is more or less the same and the strength is slightly lower in the recycled sample, due to the extremely harsh conditions of the recycling process. These tests conditions also affect the statistical dispersion of the results in the recycled samples, being slightly higher.

4. Conclusions

Lanthanide triflates can be used as Lewis acid catalysts to prepare crosslinked poly(thiourethane)s and catalysts in the vitrimeric relaxation of these materials. The different sizes, coordination abilities, and Lewis acidities of the lanthanide cations lead to gradual differences.

The curing process consists of two distinct reactions: the first, at moderate temperatures, is the formation of isocyanurate rings by isocyanate trimerization, which occurs to a greater extent as the size of the lanthanide cation increases. The second process, the formation of thiourethane groups, occurs at higher temperatures ranging from lanthanum to ytterbium. There are no remaining isocyanurates in the final materials, but only thiourethane groups.

The T_gs of PTU networks decrease from lanthanum to ytterbium and are slightly lower than those obtained with DBTDL as the catalyst.

Two isocyanates, HDI and IPDI, were selected as starting compounds that reacted with a trithiol, S3. HDI showed a greater reactivity than IPDI, but the last led to higher T_gs of the final material due to its rigid structure.

Materials prepared with lanthanum salt begin to degrade at temperatures slightly lower than those obtained with DBTDL but are sufficiently stable to be recycled at temperatures below 200 °C.

Using DBTDL as the catalyst leads to the highest tan δ temperature, and among lanthanide triflates, the ytterbium salt leads to the lowest. Using lanthanide triflates leads to materials with slightly higher storage moduli, especially for the lanthanum catalyst. On increasing the

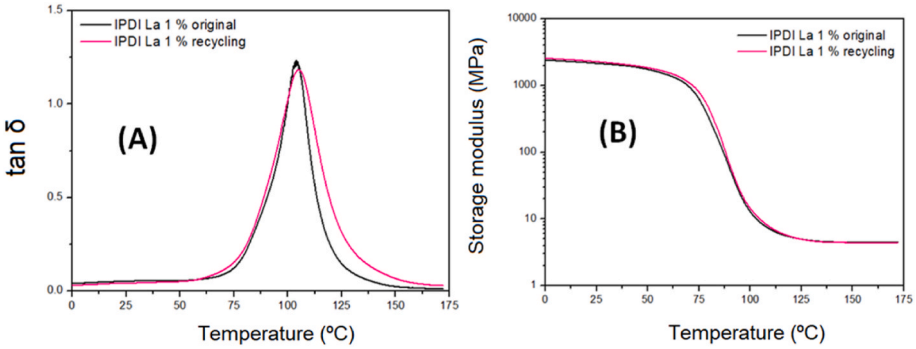

Fig. 13. Plots of tan δ and storage moduli evolution with temperature of the original IPDI 1% La and after the recycling process.

Table 5
Main data extracted from tensile test at break for original and recycled sample.

Sample	Stress at break (MPa)	Strain at break (%)	Tensile Modulus (MPa)
IPDI La 1%-original	28.8 ± 5.4	1.24 ± 0.3	2083 ± 1 6
IPDI La 1%-recycled	24.2 ± 5 .8	1.21 ± 0.8	1927 ± 57

proportion of lanthanum triflate in the material, tan δ temperature remains unchanged with bare changes in their rigidity.

Lanthanum salt leads to the best results in stress relaxation, and even ytterbium triflate leads to faster relaxation than DBTDL. The stress relaxation rate improves noticeably by increasing the lanthanum triflate proportion in the formulation. The rigidity of IPDI, in contrast to the flexibility of HDI, slows down the stress relaxation process.

The evolution of the viscosity of the materials with lanthanide triflates against time at high temperatures follows an Arrhenius evolution. It helps to assert that the PTUs prepared with lanthanide triflates have a vitrimer-like behavior. Lanthanum salt leads to the lowest topology freezing transition temperature, which decreases by increasing the amount of catalyst.

The materials can be recycled without differences in their structure, and the thermomechanical and mechanical properties remain unchanged after the recycling processes, with only slight differences due to statistical dispersion.

CRediT authorship contribution statement

Federico Guerrero: performed the experimental part, wrote the article. **Francesco Gamardella:** performed the experimental part. **Xavier Ramis:** conceived and designed the experiments, All the authors analyzed the data and discussed the results, revised it, All authors have read and agreed to the published version of the manuscript. **Silvia De la Flor:** Conceptualization, and designed the experiments, revised it. **Àngels Serra:** Conceptualization, and designed the experiments.

Declaration of competing interest

The authors declare that they have no known competing financial interests or personal relationships that could have appeared to influence the work reported in this paper.

Data availability

Data will be made available on request.

Acknowledgments

This work is part of the R&D projects PID2020-115102RB-C21 and PID2020-115102RB-C22 funded by MCNI/AEI/10.13039/501100011033. We acknowledge these grants and to the Generalitat de Catalunya (2021-SGR-00154 and BASE3D). F.G. thanks to MCNI/AEI for the grant PRE2018-084192.

References

[1] J.H. Forsberg, V.T. Spaziano, T.M. Balasubramanian, G.K. Liu, S.A. Kinsley, C. A. Duckworth, J.J. Poteruca, P.S. Brown, J.L. Miller, Use of lanthanide(III) ions as catalysts for the reactions of amines with nitriles, J. Org. Chem. 52 (1987) 1017–1021, https://doi.org/10.1021/jo00382a009.
[2] S. Hirano, K.T. Suzuki, Exposure, metabolism, and toxicity of rare earths and related compounds, Environ. Health Perspect. 104 (1996) 85–95, https://doi.org/10.2307/3432699.
[3] S. Kobayashi, Rare earth metal trifluoromethanesulfonates as water-tolerant Lewis acid catalysts in organic synthesis, 1994, Synlett (1994) 689–701, https://doi.org/10.1055/s-1994-22976.
[4] C.G. Fortuna, G. Musumarra, M. Nardi, A. Procopio, G. Sindona, S. Scirè, Principal properties (PPs) for lanthanide triflates as Lewis-acid catalysts, J. Chemometr. 20 (2006) 418–424, https://doi.org/10.1002/cem.1016.
[5] C. Huang (Ed.), Rare Earth Coordination Chemistry. Fundamentals and Applications, John Wiley & Sons, Singapore, 2010.
[6] H. Tsuruta, T. Imamoto, K. Yamaguchi, Evaluation of the relative Lewis acidities of lanthanoid(III) compounds by tandem mass spectrometry, Chem. Commun. (1999) 1703–1704, https://doi.org/10.1039/A905569J.
[7] N. Nomura, A. Taira, A. Nakase, T. Tomioka, M. Okada, Ring-opening polymerization of lactones by rare-earth metal triflates and by their reusable system in ionic liquids, Tetrahedron 63 (2007) 8478–8484, https://doi.org/10.1016/j.tet.2007.05.073.
[8] F. Hu, S. Xie, L. Jiang, Z. Shen, Living cationic ring-opening polymerization of 2-oxazolines initiated by rare-earth metal triflates, RSC Adv. 4 (2014) 59917–59926, https://doi.org/10.1039/C4RA11404C.
[9] L. You, T.E. Hogen-Esch, Y. Zhu, J. Ling, Z. Shen, Brønsted acid-free controlled polymerization of tetrahydrofuran catalyzed by recyclable rare earth triflates in the presence of epoxides, Polymer 53 (2012) 4112–4118, https://doi.org/10.1016/j.polymer.2012.07.047.
[10] P. Castell, M. Galià, A. Serra, J.M. Salla, X. Ramis, Study of lanthanide triflates as new curing initiators for DGEBA, Polymer 41 (2000) 8465–8474, https://doi.org/10.1016/S0032-3861(00)00275-5.
[11] C. Mas, A. Serra, A. Mantecón, J.M. Salla, X. Ramis, Study of lanthanide triflates as new curing initiators for cycloaliphatic epoxy resins, Macromol. Chem. Phys. 202 (2001) 2554–2564, https://doi.org/10.1002/1521-3935(20010801)202:12<2554::AID-MACP2554>3.0.CO;2-C.
[12] M. Arasa, X. Ramis, J.M. Salla, A. Mantecón, A. Serra, A study of the degradation of ester-modified epoxy resins obtained by cationic copolymerization of DGEBA with γ-lactones initiated by rare earth triflates, Polym. Degrad. Stabil. 92 (2007) 2214–2222, https://doi.org/10.1016/j.polymdegradstab.2007.01.037.
[13] S. González, X. Fernández-Francos, J. Maria Salla, A. Serra, A. Mantecón, X. Ramis, New thermosets obtained by cationic copolymerization of DGEBA with γ-caprolactone with improvement in the shrinkage. II. Time–temperature–transformation (TTT) cure diagram, J. Appl. Polym. Sci. 104 (2007) 3406–3416, https://doi.org/10.1002/app.26021.
[14] S. Kobayashi, M. Sugiura, H. Kitagawa, W.W.-L. Lam, Rare-Earth metal triflates in organic synthesis, Chem. Rev. 102 (2002) 2227–2302, https://doi.org/10.1021/cr010289i.
[15] X. Feng, Z. Wang, X. Liu, Chiral Lewis acid rare-earth metal complexes in enantioselective catalysis, in: K. Mikami (Ed.), Chiral Lewis Acids, Springer International Publishing, Cham, 2018, pp. 147–191, https://doi.org/10.1007/3418_2017_1.

[16] H.-W. Engels, H.-G. Pirkl, R. Albers, R.W. Albach, J. Krause, A. Hoffmann, H. Casselmann, J. Dormish, Polyurethanes: versatile materials and sustainable problem solvers for today's challenges, Angew. Chem. Int. Ed. 52 (2013) 9422–9441, https://doi.org/10.1002/anie.201302766.
[17] K. Strzelec, N. Bączek, S. Ostrowska, K. Wąsikowska, M.I. Szynkowska, J. Grams, Synthesis and characterization of novel polythiourethane hardeners for epoxy resins, Compt. Rendus Chim. 15 (2012) 1065–1071, https://doi.org/10.1016/j.crci.2012.09.003.
[18] Q. Li, H. Zhou, D.A. Wicks, C.E. Hoyle, D.H. Magers, H.R. McAlexander, Comparison of small molecule and polymeric urethanes, thiourethanes, and dithiourethanes: hydrogen bonding and thermal, physical, and mechanical properties, Macromolecules 42 (2009) 1824–1833, https://doi.org/10.1021/ma802848t.
[19] B. Jaffrennou, N. Droger, F. Méchin, J.-L. Halary, J.-P. Pascault, Characterization, structural transitions and properties of a tightly crosslinked polythiourethane network for optical applications, E-Polymers 5 (2005), https://doi.org/10.1515/epoly.2005.5.1.866.
[20] A.B. Lowe, C.N. Bowman, Thiol-X Chemistries in Polymer and Materials Science, RSC Publishing, Cambridge, UK, 2013.
[21] J. Shin, H. Matsushima, C.M. Comer, C.N. Bowman, C.E. Hoyle, Thiol−Isocyanate−Ene ternary networks by sequential and simultaneous thiol click reactions, Chem. Mater. 22 (2010) 2616–2625, https://doi.org/10.1021/cm903856n.
[22] S. Huang, M. Podgórski, X. Han, C.N. Bowman, Chemical recycling of poly (thiourethane) thermosets enabled by dynamic thiourethane bonds, Polym. Chem. 11 (2020) 6879–6883, https://doi.org/10.1039/D0PY01050B.
[23] S. Kuypers, S.K. Pramanik, L. D'Olieslaeger, G. Reekmans, M. Peters, J. D'Haen, D. Vanderzande, T. Junkers, P. Adriaensens, A. Ethirajan, Interfacial thiol–isocyanate reactions for functional nanocarriers: a facile route towards tunable morphologies and hydrophilic payload encapsulation, Chem. Commun. 51 (2015) 15858–15861, https://doi.org/10.1039/C5CC05258K.
[24] H. Salmi, X. Allonas, C. Ley, Polythiourethane networks catalyzed by photobase generators, Prog. Org. Coating 100 (2016) 81–85, https://doi.org/10.1016/j.porgcoat.2016.03.017.
[25] F. Gamardella, X. Ramis, S. De la Flor, À. Serra, Preparation of poly(thiourethane) thermosets by controlled thiol-isocyanate click reaction using a latent organocatalyst, React. Funct. Polym. 134 (2019) 174–182, https://doi.org/10.1016/j.reactfunctpolym.2018.11.019.
[26] Y. Jia, B. Shi, J. Jin, J. Li, High refractive index polythiourethane networks with high mechanical property via thiol-isocyanate click reaction, Polymer 180 (2019), 121746, https://doi.org/10.1016/j.polymer.2019.121746.
[27] C. Lü, C. Guan, Y. Liu, Y. Cheng, B. Yang, PbS/Polymer nanocomposite optical materials with high refractive index, Chem. Mater. 17 (2005) 2448–2454, https://doi.org/10.1021/cm050113n.
[28] F. Gamardella, F. Guerrero, S. De la Flor, X. Ramis, A. Serra, A new class of vitrimers based on aliphatic poly(thiourethane) networks with shape memory and permanent shape reconfiguration, Eur. Polym. J. 122 (2020), 109361, https://doi.org/10.1016/j.eurpolymj.2019.109361.
[29] https://echa.europa.eu/documents/10162/037ff6ad-39d0-d73d-b042-9f9c47bb410f. (Accessed 5 April 2023).
[30] F. Guerrero, X. Ramis, S. de la Flor, À. Serra, Preparation of poly(thiourethane) networks by using a novel acidic organocatalyst. Evaluation of their vitrimer-like behavior, React. Funct. Polym. 183 (2023), 105501, https://doi.org/10.1016/j.reactfunctpolym.2023.105501.
[31] H. Li, B. Yu, H. Matsushima, C.E. Hoyle, A.B. Lowe, The Thiol−Isocyanate click reaction: facile and quantitative access to ω-end-functional poly(N,N-diethylacrylamide) synthesized by RAFT radical polymerization, Macromolecules 42 (2009) 6537–6542, https://doi.org/10.1021/ma9010878.
[32] F.J. Waller, A.G.M. Barrett, D.C. Braddock, R.M. McKinnell, D. Ramprasad, Lanthanide(III) and Group IV metal triflate catalysed electrophilic nitration: 'nitrate capture' and the rôle of the metal centre, J. Chem. Soc., Perkin Trans. 1 (1999) 867–871.
[33] F. Gamardella, S. Muñoz, S. De la Flor, X. Ramis, A. Serra, Recyclable organocatalyzed poly(thiourethane) covalent adaptable networks, Polymers 12 (2020) 2913, https://doi.org/10.3390/polym12122913.
[34] S. Cotton, Lanthanide and Actinide Chemistry, John Wiley & Sons, Chichester, UK, 2006.
[35] S.A. Cotton, Establishing coordination numbers for the lanthanides in simple complexes, Compt. Rendus Chem. 8 (2005) 129–145, https://doi.org/10.1016/j.crci.2004.07.002.
[36] M. Flores, X. Fernández-Francos, J.M. Morancho, À. Serra, X. Ramis, Ytterbium triflate as a new catalyst on the curing of epoxy–isocyanate based thermosets, Thermochim. Acta 543 (2012) 188–196, https://doi.org/10.1016/j.tca.2012.05.012.
[37] G. Trovati, E.A. Sanches, S.C. Neto, Y.P. Mascarenhas, G.O. Chierice, Characterization of polyurethane resins by FTIR, TGA, and XRD, J. Appl. Polym. Sci. 115 (2010) 263–268, https://doi.org/10.1002/app.31096.
[38] F. Gamardella, S. De la Flor, X. Ramis, A. Serra, Recyclable poly(thiourethane) vitrimers with high Tg. Influence of the isocyanate structure, React. Funct. Polym. 151 (2020), 104574, https://doi.org/10.1016/j.reactfunctpolym.2020.104574.
[39] E. Delebecq, J.-P. Pascault, B. Boutevin, F. Ganachaud, On the versatility of urethane/urea bonds: reversibility, blocked isocyanate, and non-isocyanate polyurethane, Chem. Rev. 113 (2013) 80–118, https://doi.org/10.1021/cr300195n.